ARTICLE

pubs.acs.org/Biomac

Galactose-Decorated Cross-Linked Biodegradable Poly(ethylene glycol)-*b*-poly(ε-caprolactone) Block Copolymer Micelles for Enhanced Hepatoma-Targeting Delivery of Paclitaxel

Rui Yang,[†] Fenghua Meng,[†] Shoubao Ma,[‡] Fushi Huang,[†] Haiyan Liu,[‡] and Zhiyuan Zhong*[,†]

[†]Biomedical Polymers Laboratory, and Jiangsu Key Laboratory of Advanced Functional Polymer Design and Application, Department of Polymer Science and Engineering, College of Chemistry, Chemical Engineering and Materials Science, Soochow University, Suzhou, 215123, P. R. China.

[‡]Laboratory of Cellular and Molecular Tumor Immunology, Institute of Biology and Medical Sciences, Soochow University, Suzhou 215123, P. R. China

ABSTRACT:

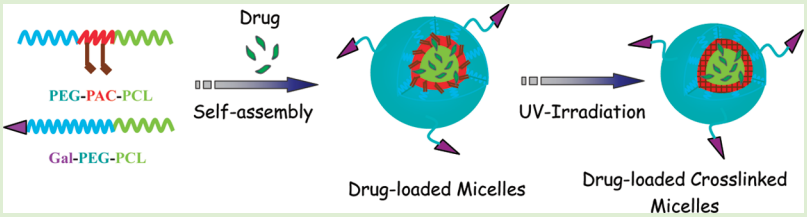

The inferior in vivo stability of micellar drugs has been a prime challenge for their application in targeted drug delivery. Here we report on novel galactose-decorated covalently cross-linked biodegradable micelles based on photo-cross-linkable poly(ethylene glycol)-*b*-poly(acryloyl carbonate)-*b*-poly(ε-caprolactone) (PEG-PAC-PCL) and galactose-conjugated PEG-PCL (Gal-PEG-PCL) copolymers for enhanced hepatoma-targeting delivery of paclitaxel (PTX). The molecular weight of PEG in Gal-PEG-PCL was higher than that in PEG-PAC-PCL, thereby fully exposing Gal ligands at the micellar surface. These micelles, either with or without loading of PTX, were readily cross-linked by UV irradiation to afford micelles with small sizes (ca. 79−94 nm) and enhanced stability. The in vitro release studies confirmed that drug release from cross-linked micelles was significantly inhibited. Interestingly, MTT assays showed that Gal-decorated PTX-loaded cross-linked micelles retained a high antitumor activity in HepG2 cells, which was much more effective than PTX-loaded cross-linked micelles without Gal ligands and comparable to Gal-decorated PTX-loaded non-cross-linked micelles. Remarkably, the preliminary in vivo antitumor efficacy studies in SMMC-7721 tumor (human hepatoma)-bearing nude mice revealed that Gal-decorated PTX-loaded cross-linked micelles inhibited the growth of the human hepatoma more effectively than PTX-loaded cross-linked micelles as well as Gal-decorated PTX-loaded non-cross-linked micelles. These results indicate that Gal-decorated cross-linked PEG-PCL micelles have great potential in liver tumor-targeted chemotherapy.

INTRODUCTION

In recent years, polymeric micelles have emerged as one of the most promising carrier systems for poorly water-soluble anticancer drugs including clinically widely applied doxorubicin (DOX) and paclitaxel (PTX).[1−3] They offer several advantages such as significantly enhancing drug water solubility, prolonging circulation time, targeting to the tumor tissues via the enhanced permeability and retention (EPR) effect, decreasing side effects, and improving drug bioavailability.[1,4,5] In particular, biodegradable micelles based on block copolymers of poly(ethylene glycol) (PEG) and aliphatic biodegradable polyesters such as polylactide (PLA), poly(lactide-*co*-glycolide) (PLGA), and poly(ε-caprolactone) (PCL) are among the most studied.[6−9] Notably, a couple of micellar anticancer drug formulations, for example, NK911 and Genexol-PM, have already advanced to the clinical trials.[10,11]

In the past decade, biodegradable micelles have been designed with different targeting ligands including folic acid, antibody, peptide, or galactose/lactose for tumor cell specific delivery of chemotherapeutics.[12,13] For example, Gao et al. reported that attachment of cyclic RGD ligand greatly enhances internalization of the PEG-*b*-PCL micelles in tumor endothelial cells overexpressing $\alpha v\beta 3$ integrins.[14] Park et al. reported that folate-conjugated DOX-loaded PEG-*b*-PLGA micelles are far more efficiently uptaken by KB cells than corresponding DOX-loaded micelles without folate ligand.[15] Kim et al. reported that anti-epidermal growth factor receptor antibody (anti-EGFR antibody)-conjugated PEG-PCL micelles result in enhanced delivery of DOX to EGFR overexpressing RKO cells.[16] The asialoglycoprotein receptor (ASGP-R) on mammalian hepatocytes that specifically recognizes β-D-galactose, *N*-acetylgalactosamine, and lactose ligands provides a unique means for the development of liver-targeted drug delivery systems. For example, Hsiue et al. reported

Received: May 19, 2011
Revised: June 30, 2011
Published: July 05, 2011

dx.doi.org/10.1021/bm2006856 | *Biomacromolecules* 2011, 12, 3047–3055

Scheme 1. Illustration on the Preparation of Galactose-Decorated Interfacially Crosslinked Biodegradable Micelles from PEG-PAC-PCL and Gal-PEG-PCL Block Copolymers, Followed by UV Irradiation

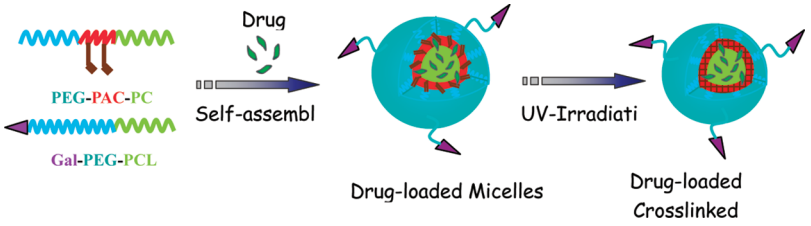

that galactosamine-conjugated multifunctional micelles deliver DOX to HepG2 cells via a receptor-mediated targeting mechanism.[17] Zhang et al. reported that galactosylated FITC-labeled dextran-*g*-PCL micelles exhibit apparent targetability to HepG2 cells and liver tissue.[18]

However, one remaining practical challenge for micellar drugs is their inferior in vivo stability.[3,19,20] In the past several years, various cross-linking approaches have been adopted to improve micellar stability.[3,20−22] The cross-linking of micelles could take place on the hydrophilic shell,[23−25] within the hydrophobic core,[26−30] or at the core−shell interface.[31,32] It should be noted, nevertheless, that there are only a few reports on the development of cross-linked biodegradable micelles for anticancer drug delivery. For example, Kissel et al. reported that core-cross-linked PEG-PCL micelles exhibited significantly enhanced PTX-loading efficiency and thermodynamic stability against dilution.[33] Hennink et al. reported that core-cross-linked micelles based on PEG-*b*-p(HPMAm-Lac$_n$) had prolonged circulation time and much higher accumulation in the tumor than the non-cross-linked micelles (NCLMs),[27] and pH-activatable DOX-conjugated core-cross-linked micelles led to better antitumor activity in B16F10-bearing mice than free DOX.[30] The conjugation of anti-EGFR nanobody to core-cross-linked micelles was reported to enhance substantially the binding as well as uptake by EGFR overexpressing cancer cells.[34] We reported that interfacially cross-linked PEG-PCL micelles retained most drugs, even at concentrations close to the CMC, whereas NCLMs released DOX rapidly under otherwise the same conditions.[31] We reported recently that folate-conjugated photo-cross-linkable PEG-PLA micelles had higher drug loading, enhanced stability, and improved uptake by KB cells.[35] It should be noted that despite some progress made with cross-linked micelles (CLMs), there is no report on the in vivo targetability and therapeutic evaluation of ligand-conjugated cross-linked biodegradable micelles.

In this Article, we report on novel galactose-decorated interfacially cross-linked biodegradable PEG-PCL block copolymer micelles for enhanced hepatoma-targeting delivery of PTX. The micelles were prepared from photo-cross-linkable PEG-*b*-poly(acryloyl carbonate)-*b*-PCL (PEG-PAC-PCL) triblock copolymer and galactose-conjugated PEG-PCL (Gal-PEG-PCL) diblock copolymer at varying Gal-PEG-PCL contents from 0 to 20 wt %, followed by UV irradiation (Scheme 1). Interestingly, our results revealed that these Gal-decorated CLMs have improved stability with inhibited release of PTX upon dilution, superior hepatoma targetability, and enhanced in vivo antitumor efficacy.

EXPERIMENTAL SECTION

Materials. Methoxy poly(ethylene glycol) (PEG, M_n = 5000 g/mol, Fluka) was dried by azeotropic distillation from anhydrous toluene. ε-Caprolactone (ε-CL, 99%, Alfa Aesar) was dried over CaH_2 and distilled under reduced pressure prior to use. Allyl alcohol (98%, shanghai) was dried with anhydrous magnesium sulfate and distilled under reduced pressure. Dichloromethane (DCM) and dimethyl sulfoxide (DMSO) were dried by refluxing over CaH_2 and distilled prior to use. Zinc bis[bis[trimethylsilyl]-amide] (97%, Aldrich), lactobionic acid (LBA, 97%, Acros), cystamine dihydrochloride (>98%, Alfa Aesar), 1-[4-(2-hydroxy ethoxy)-phenyl]-2-hydroxy-2-methyl-1-propanone (Irgacure 2959 or I2959, 98%, Sigma), paclitaxel (PTX, >99%, Beijing Zhongshuo Pharmaceutical Technology Development), fluorescein isothiocyanate (FITC, 98%, Sigma), triethylamine (TEA, 99%, Alfa Aesar), 1-(3-dimethylaminopropyl)-3-ethylcarbodiimide hydrochloride (EDC, 98%, J&K), and *N*-hydroxysuccinimide (NHS, 98%, Alfa Aesar) were used as received. Acryloyl carbonate (AC) monomer was synthesized according to a previous report.[36] Spectra/Pore dialysis membranes (MWCO 3500 and 12 000−14 000) were purchased from Spectrum Laboratories.

Characterization. The ^{1}H NMR spectra were recorded on a Unity Inova 400 spectrometer operating at 400 MHz using deuterated chloroform ($CDCl_3$) or deuterated dimethylsulfoxide (DMSO-d_6) as a solvent. The chemical shifts were calibrated against residual solvent signals. The molecular weight and polydispersity of the copolymers were determined by a Waters 1515 gel permeation chromatograph (GPC) instrument equipped with two linear PLgel columns (500 Å and Mixed-C) following a guard column and a differential refractive-index detector. The measurements were performed using THF as an eluent at a flow rate of 1.0 mL/min at 30 °C and a series of narrow polystyrene standards for the calibration of the columns. The surface charge and size of micelles were measured in phosphate buffer (10 mM, pH 7.4) at 25 °C with a Zetasizer Nano ZS instrument (Malvern) equipped with a standard capillary electrophoresis cell and dynamic light scattering (DLS, 10 mW He−Ne laser, 633 nm wavelength), respectively. The data were analyzed using the associated Zetasizer software (Dispersion Technology Software v 5.00; Malvern). The average hydrodynamic size of micelles was obtained based on the Stokes−Einstein equation. The viscosity and refractive index of water were used. The measurements were performed in triplicate. The SEM images of the micelles were taken on a Hitachi S-4700 scanning electron microscope. The amount of PTX was determined by HPLC (Waters 1525) with UV detection at 227 nm using acetonitrile/water (1/1 v/v) as a mobile phase.

Synthesis of PEG-PAC-PCL Triblock Copolymer. Under a N_2 atmosphere, to a solution of PEG (0.47 g, 0.094 mmol) and AC (0.15 g, 0.75 mmol) in DCM (4 mL) was added with stirring a solution of zinc bis[bis(trimethylsilyl)amide] (0.018 g, 0.047 mmol). The reaction proceeded at room temperature (r.t.) for 2 days. Then, the second monomer, ε-CL (0.32 g, 2.8 mmol), in 2 mL of DCM was added. The reaction was allowed to proceed at 30 °C for an additional 2 days before termination with acetic acid. The resulting PEG-PAC-PCL copolymer was isolated by precipitation in cold diethyl ether, filtration, and drying in vacuo for 2 days. Yield: 78%, M_n (GPC) = 12 000 g/mol, PDI (GPC) = 1.6.

Synthesis of Allyl-PEG -PCL Diblock Copolymer. Allyl-PEG-PCL was synthesized by sequential anionic ring-opening polymerization of EO and ε-CL in one pot using allyl alcohol/potassium naphthalene as

an initiator system. Under a N_2 atmosphere, EO (2.26 g, 51 mmol) was added with stirring to a solution of potassium naphthalene (0.546 g, 3.12 mmol), allyl alcohol (0.023 g, 0.40 mmol), and 18-crown-6 (0.075 g, 0.28 mmol) in THF (6 mL) at 0 °C. The polymerization was conducted at 35 °C for 3 days. Then, one sample was taken for measurements. To the rest of the reaction mixture was added a solution of ε-CL (1.88 g, 16.5 mmol) in THF (2 mL). The reaction was allowed to proceed at 40 °C for additional 2 days before termination with acetic acid. The resulting copolymer was isolated by precipitation in hexane, dissolving in DCM and reprecipitation in cold diethyl ether, filtration, washing with diethyl ether, and drying in vacuo for 2 days. Yield: 86%. M_n (GPC) = 10 800 g/mol, PDI (GPC) = 1.3.

Synthesis of NH_2-PEG-PCL. Under a N_2 atmosphere, to a 25 mL reaction vessel equipped with a magnetic stirrer was introduced allyl-PEG-PCL (2.39 g, 0.239 mmol), cysteamine hydrochloride (0.57 g, 4.97 mmol), AIBN (0.47 g, 2.89 mmol), and dry DMF (30 mL). The mixture was stirred at 70 °C for 24 h. The product, amine-PEG-PCL, was isolated by precipitation in cold diethyl ether, filtration, and drying in vacuo for 2 d. Yield: 85%.

Synthesis of Gal-PEG-PCL. Gal-PEG-PCL was synthesized by carbodiimide chemistry. The coupling reaction of NH_2-PEG-PCL (2 g, mmol) and LBA (0.196 g, 0.55 mmol) was carried out under stirring for 24 h in DMSO (60 mL) in the presence of NHS (0.095 g, 0.83 mmol), EDC (0.31 g, 1.62 mmol), and TEA (0.76 mL, 7.5 mmol). The product was isolated by filtration through a number-4 sintered glass funnel to remove 1,3-dicyclohexylurea (DCU), dialysis against DMSO for 48 h and deionized water for another 48 h (MWCO 3500), and freeze-drying. The degree of Gal conjugation was determined by ^{1}H NMR. Yield: 77%.

Formation of Micelles and Critical Micelle Concentration Determination. Micelles were prepared by dropwise addition of 4 mL of phosphate buffer (PB, pH 7.4, 10 mM) to a DMF solution (1 mL) of PEG-PAC-PCL or PEG-PAC-PCL/Gal-PEG-PCL mixture (5 mg/mL) under stirring at r.t., followed by ultrasonication for 30 min and extensive dialysis (MWCO 3500) against PB (pH 7.4, 10 mM).

The critical micelle concentration (CMC) was determined using pyrene as a fluorescence probe. The concentration of block copolymer was varied from 6.0×10^{-4} to 0.15 mg/mL, and the concentration of pyrene was fixed at 1.0 μM. The fluorescence spectra were recorded using an Edinburgh FLS920 fluorometer (Edinburgh Instrument) with the excitation wavelength of 330 nm. The emission fluorescence at 372 and 383 nm was monitored. The CMC was estimated as the cross-point when extrapolating the intensity ratio I_{372}/I_{383} at low and high concentration regions.

UV Cross-Linking of PEG-PAC-PCL Containing Micelles. The biocompatible UV initiator, 1-[4-(2-hydroxyethoxy)-phenyl]-2-hydroxy-2-methyl-1-propanone (Irgacure 2959 or I2959), which has been widely used to prepare photo-cross-linked hydrogels for cell encapsulation and tissue engineering,[37] was employed as a photoinitiator to cross-link the micelles at the interface. Acetone solution of I2959 (25 μL, 10 mg/mL) was introduced to a micelle solution of PEG-PAC-PCL or PEG-PAC-PCL/Gal-PEG-PCL (1 mL, 0.6 mg/mL), resulting in a final I2959 concentration of 0.025 wt.%. The mixture was ultrasonicated for 1 h to evaporate acetone. Then, the micelle solution was irradiated under the UV light (Intelli-Ray 400, Uvitron) at 100 mW/cm^2 for 10 min to yield CLMs. The CLMs and the corresponding NCLMs were studied in terms of size, morphology, and stability against extensive dilution and physiological salt concentration.

Preparation of FITC-Labeled Gal-Functionalized Micelles. The micelles were prepared as described above from a mixture of PEG-PAC-PCL (0.4 mL, 5 mg/mL), Gal-PEG-PCL (0.16 mL, 5 mg/mL), and NH_2−PEG-PCL (0.24 mL, 5 mg/mL). The micelles were cross-linked by UV irradiation. FITC was conjugated to the micelles by treating micelles (4 mL, 0.76 mg/mL) with FITC (0.12 mg, 0.3 μmol) under the dark at pH 8.5 and r.t. for 20 h. Free FITC was removed by dialysis against PB (10 mM, pH 7.4). The conjugation amount of FITC was quantified by fluorescence using a Edinburgh FLS920 fluorometer (Edinburgh Instrument).

Loading of PTX into Micelles. PTX-loaded micelles were prepared by dropwise addition of 4 mL of PB (10 mM, pH 7.4) to a mixture of copolymer (1 mL, 5 mg/mL) and PTX (50 μL, 5 mg/mL) in DMF under stirring at r.t., followed by dialysis against PB (10 mM, pH 7.4) for 8 h at r.t (Spectra/Pore dialysis membrane, MWCO 3500, Spectrum Laboratories). The dialysis medium was changed five times. The micelles were cross-linked, as described above by UV irradiation. Drug loading content (DLC) and drug loading efficiency (DLE) were determined as previously described.[38] The drug loaded in the micelles was extracted using acetonitrile, and the amount of PTX was determined by HPLC (Waters 1525) with UV detection at 227 nm using a 1/1 (v/v) mixture of acetonitrile and water as a mobile phase. DLC and DLE were calculated according to the following formula:

$$\text{DLC (wt \%)} = [\text{weight of loaded drug}/(\text{weight of loaded drug} + \text{weight of polymer})] \times 100\%$$

$$\text{DLE (\%)} = (\text{weight of loaded drug}/\text{weight of drug in feed}) \times 100\%$$

In Vitro Release of PTX from the Micelles. The release behaviors of PTX from the cross-linked and NCLMs were studied in PB (10 mM, pH 7.4) using a dialysis method (Spectra/Pore dialysis membrane, MWCO 12 000−14 000, Spectrum Laboratories) at 37 °C at different micelle concentrations. PTX loaded cross-linked or NCLMs were divided into two groups: one at a concentration of 0.75 mg/mL and the other at 0.075 mg/mL (i.e., 10 times dilution). PTX-loaded micelle solutions (1 mL) were then immediately transferred to dialysis tubes, which were immersed in 25 mL of PB (pH 7.4, 10 mM). The release studies were performed under constant shaking at 37 °C. At desired time intervals, 7 mL of release media was taken for HPLC measurement and replenished with an equal volume of fresh media. The amount of PTX was determined by HPLC (Waters 1525) with UV detection at 227 nm using a 1/1 (v/v) mixture of acetonitrile and water as a mobile phase. The release experiments were conducted in triplicate. The results presented are the average data with standard deviations. 1.

MTT Assays. HepG2 cells were plated in a 96-well plate (1×10^4 cells/well) using RPMI-1640 medium supplemented with 10% fetal bovine serum, 1% L-glutamine, antibiotics penicillin (100 IU/mL), and streptomycin (100 μg/mL) for 24 h to reach 70% confluence. The cells were incubated with PTX-loaded CLMs, PTX-loaded non-crosslinked micelles, and free PTX (drug dosage 6 μg/mL), respectively, at 37 °C in an atmosphere containing 5% CO_2 for 1 or 3 days. Then, 10 μL of 3-(4,5-dimethylthiazol-2-yl)-2,5-diphenyltetrazoliumbromide (MTT) solution in PBS (5 mg/mL) was added and incubated for another 4 h. The medium was aspirated, the MTT-formazan generated by live cells was dissolved in 150 μL of DMSO, and the absorbance at a wavelength of 490 nm of each well was measured using a microplate reader (Biorad, ELX808 IU). The cell viability (%) was determined by comparing the absorbance at 490 nm with control wells containing only cell culture medium. Data are presented as average ± SD (n = 4).

Flow Cytometry Analysis on Cellular Uptake of FITC-Labeled Micelles. HepG2 cells were seeded onto 24-well plates at 1×10^5 cells per well (1 mL) for 24 h. FITC-labeled micelles with or without Gal ligands were added. After incubation at 37 °C for 12 or 24 h, the cells were digested by 0.25 w/v% trypsin/0.03 w/v% EDTA. The suspensions were centrifuged at 1000g for 4 min at 4 °C, pelleted in eppendorf tubes, washed twice with cold PBS, and then resuspended in 500 μL of PBS with 2% FBS. Fluorescence histograms were recorded with a BD FACSCalibur (Beckton Dickinson) flow cytometer and analyzed using Cell Quest software. We analyzed 20 000 gated events

Scheme 2. Synthesis of PEG-PAC-PCL Triblock Copolymer by Sequential Ring-Opening Polymerization of Acryloyl Carbonate (AC) and ε-Caprolactone (CL) Using Methoxy PEG As an Initiator, Zinc Bis[bis(trimethylsilyl)amide] As a Catalyst, and CH_2Cl_2 As a Solvent[a]

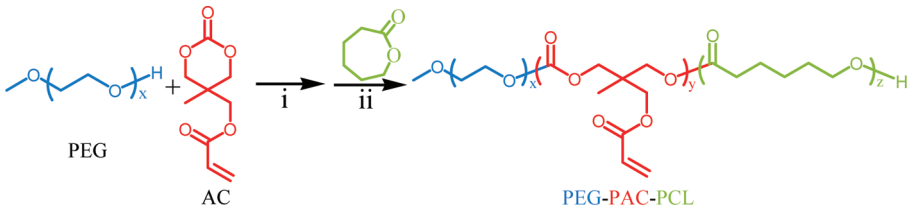

[a] Conditions: (i) r.t., 2 days and (ii) 30 °C, 2 days.

to generate each histogram. The gate was arbitrarily set for the detection of green fluorescence.

In Vivo Antitumor Efficacy of PTX-Loaded Micelles. The in vivo antitumor efficacy of PTX-loaded micelles was evaluated using the nude mice implanted with human hepatocellular carcinoma (SMMC-7721). The mice were handled under protocols approved by Soochow University Laboratory Animal Center. Nude mice (18−22 g) were injected subcutaneously in the armpit of right posterior limb with 0.2 mL of cell suspension containing 5×10^6 SMMC-7721 cells. Treatments were started after 2 weeks when tumor in the nude mice reached a tumor volume of 27−50 mm^3, and this day was designated as day 0. The mice were weighed and randomly divided into four groups of four mice: (i) group 1: PBS (blank control); (ii) group 2: PTX-loaded CLMs (PTX-CLM); (iii) group 3: Gal decorated PTX-loaded NCLMs (Gal-PTX-NCLM); and (iv) group 4: Gal decorated PTX-loaded CLMs (Gal-PTX-CLM). A single i.v. dose of PTX-loaded micelles in 0.2 mL of PBS (PTX dosage was set at 3 mg/kg body weight) or 0.2 mL of PBS alone was intravenously administrated via the tail vein on days 0 and 7. The treatment effect was assessed by measuring the tumor size. Tumor volume was calculated by the formula: $V = 0.5 \times L \times W^2$, wherein L is the tumor dimension at the longest point and W is the tumor measurement at the widest point. On day 23, all mice were sacrificed by cervical vertebra dislocation, and the tumor block was separated and weighted.

RESULTS AND DISCUSSION

Synthesis of PEG-PAC-PCL Triblock Copolymer and Gal-PEG-PCL Diblock Copolymer. In this study, we were set to develop galactose-functionalized robust biodegradable PEG-PCL block copolymer micelles for hepatoma-targeting delivery of PTX, for which two copolymers, PEG-PAC-PCL triblock copolymer and Gal-PEG-PCL diblock copolymer, were designed. PEG-PAC-PCL was devised to cross-link the micelles at the interface by UV irradiation, resulting in superior micellar stability, whereas Gal-PEG-PCL was to target asialoglycoprotein receptor (ASGP-R) overexpressing hepatoma cells leading to hepatoma-specific cellular uptake. The combination of interfacial cross-linking and active targeting was hypothesized to prevent effectively premature drug release, prolong their circulation time, increase their accumulation at the tumor tissues, as well as boost their uptake by tumor cells. Notably, this novel design of micelles allowed facile control over both the extent of cross-linking and the Gal ligand density at the micellar surface.

PEG-PAC-PCL triblock copolymer was synthesized by sequential ring-opening polymerization of AC and ε-CL using PEG as an initiator and zinc bis[bis(trimethylsilyl)amide] as a catalyst in CH_2Cl_2 at 30 °C (Scheme 2). As in our previous report, AC could be readily obtained and copolymerized with other cyclic monomers.[36] ^{1}H NMR spectrum of PEG-PAC-PCL copolymer

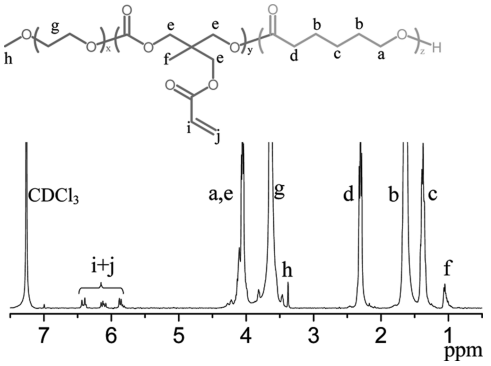

Figure 1. ^{1}H NMR spectrum (400 MHz, $CDCl_3$) of PEG-PAC-PCL copolymer.

showed signals at δ 3.63, 5.85−6.47, and 2.30 attributable to the methylene protons of PEG, the acryloyl protons of PAC, and the methylene protons neighboring to the carbonyl group of PCL, respectively (Figure 1). The molecular weights of PAC and PCL blocks were determined to be 1.2 and 3.0 kg/mol, respectively, by comparing integrals of signals at δ 5.85−6.47 and 2.30 to 3.63. GPC revealed that the resulting copolymer had a unimodal distribution with a polydispersity of 1.6 and an M_n of 12.0 kg/mol, close to the design and that determined by ^{1}H NMR (Table1, entry 1).

Gal-PEG-PCL was obtained in three steps, that is, synthesis of allyl-PEG-PCL, conversion of allyl into primary amino function, and conjugation with galactose via carbodiimide chemistry (Scheme 3). To warrant full exposure of Gal at the surface, here PEG was designed to have an M_n of 6.0 kg/mol, higher than that of PEG (M_n = 5.0 kg/mol) in PEG-PAC-PCL triblock copolymer. Allyl-PEG-PCL was obtained by sequential anionic ring-opening polymerization of ethylene oxide (EO) and ε-CL. ^{1}H NMR spectrum displayed besides signals of PEG (δ 3.63) and PCL (δ 4.10, 2.30, 1.65, and 1.35) also resonances of allyl terminal (δ 5.85−6.95 and 5.17) (Figure 2A). ^{1}H NMR end group analysis indicated that PEG and PCL blocks had M_n values of 6.0 and 4.0 kg/mol, respectively. Notably, GPC revealed a low polydispersity of 1.28 and an M_n of 10.8 kg/mol, which was in good agreement with that determined by ^{1}H NMR (Table1, entry 2). The allyl terminal was readily converted into primary amino groups by the addition of 2-aminoethanethiol in the presence of AIBN in DMF at 70 °C. ^{1}H NMR spectrum in $CDCl_3$ showed that signals attributable to the vinyl protons (δ 5.85−6.95) completely disappeared, whereas new peaks assignable to 2-aminoethanethioether moieties were detected at δ 2.9 and 3.2 (Figure 2B), indicating quantitative conversion of allyl to amine function.

Table 1. Characteristics of PEG-PAC-PCL and Gal-PEG-PCL Copolymers

entry	copolymers	M_n (kg/mol)			PDI[b]	CMC (mg/L)[c]
		design	^{1}H NMR[a]	GPC[b]		
1	PEG-PAC-PCL	5.0−1.6−4.0	5.0−1.2−3.0	12.0	1.6	3.65
2	Gal-PEG-PCL	6.0−5.0	6.0−4.0	10.8	1.3	5.70

[a] Calculated from ^{1}H NMR. [b] Determined by GPC using polystyrene standards (eluent: THF, flow rate: 1.0 mL/min, 30 °C). [c] Determined using pyrene as a fluorescence probe.

Scheme 3. Synthetic Pathway to Gal-PEG-PCL Block Copolymer[a]

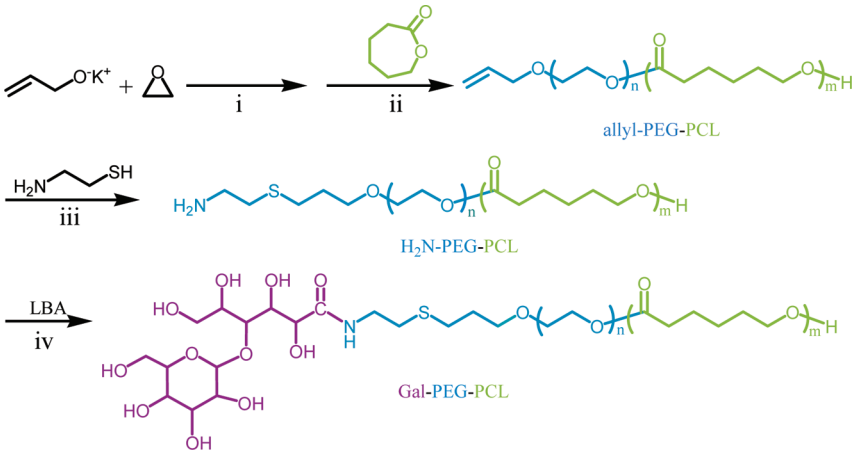

[a] Conditions: (i) THF, 35 °C, 3 days; (ii) THF, 40 °C, 2 days; (iii) DMF, AIBN, 70 °C, 1 day; and (iv) DMSO, EDC/NHS, TEA, r.t., 1 day.

Finally, LBA was attached to H_2N-PEG-PCL via carbodiimide chemistry to yield Gal-PEG-PCL. The ^{1}H NMR spectrum clearly showed signals at δ 4.17, 4.40, 4.58, 4.70, and 5.18 attributable to the LBA moieties as well as a peak at δ 5.10 assignable to the newly formed amide proton, whereas the resonance at δ 8.05 due to amine protons of H_2N-PEG-PCL completely disappeared (Figure 2C). The signals at δ 4.17 (*h*) and 4.34 (*e*), assignable to the methine proton next to the carbonyl group of LBA moieties and the last methylene protons of PEG connecting to PCL, had relative intensities corresponding to equivalent coupling. These results indicate successful synthesis of Gal-PEG-PCL.

Preparation of PTX-Loaded Interfacially Cross-Linked Micelles (PTX-CLM). Micelles were readily prepared from PEG-PAC-PCL and Gal-PEG-PCL copolymers via solvent exchange method. Dynamic light scattering (DLS) measurements showed that these micelles had average hydrodynamic sizes ranging from 87 to 115 nm depending on Gal-PEG-PCL contents (Table 2). The surface charges of these micelles were close to neutral (−1.5 ∼ +0.6 mV). The CMCs of PEG-PAC-PCL and Gal-PEG-PCL copolymers determined using pyrene as a fluorescence probe were shown to be approximately 3.65 and 5.70 mg/L, respectively (Table 1).

PEG-PAC-PCL/Gal-PEG-PCL micelles were conveniently cross-linked by UV irradiation (100 mW/cm^2) in the presence of a biocompatible photoinitiator I2959 (0.025 wt %) in PB (pH 7.4, 10 mM). The photoirradiation led to pronounced shrinkage of micelle sizes by 8−25 nm (Table 2), indicating successful cross-linking of micelles. The resulting CLMs had small average particle sizes ranging from 79 to 94 nm and low polydispersities of 0.12−0.22 (Table 2). The size distributions of CLMs containing 20 wt.% Gal-PEG-PCL (Gal-CLM) are given in Figure 3. Both DLS and SEM micrographs pointed to a homogeneous distribution of micelles. SEM revealed that Gal-CLM had a spherical morphology with an average size of ca. 65 nm (Figure 3B). Zeta potential measurements showed that all CLMs had slightly negative surface charges (−3.1 ∼ −0.9 mV) (Table 2).

PTX, a potent hydrophobic anticancer drug used widely in the treatment of different types of malignant tumors, were readily loaded into the micelles. For example, at a theoretical DLC of 9.1 wt %, high PTX loading efficiencies of 65−83% were obtained (Table 3). PTX loading efficiency decreased with increasing the amount of Gal-PEG-PCL, most likely because the addition of Gal-PEG-PCL decreases micelle cross-linking density, leading to more pronounced drug loss during preparation of PTX-loaded micelles. PTX-loaded NCLMs (PTX-NCLM) had average sizes of about 96−120 nm, which were similar to those of the corresponding empty micelles (87−115 nm, Table 2). Furthermore, the sizes of PTX-loaded CLMs (PTX-CLM) decreased by 19−28 nm upon UV irradiation (Table 3), supporting cross-linking of micelles. PTX-NCLM had close to neutral ζ potentials (−0.1 to 1.3 mV), whereas PTX-CLM displayed slightly negative surface charges (−5.3 ∼ −0.8 mV) (Table 3). These results indicate that loading of PTX has little influence on sizes, surface charges, as well as cross-linking of micelles.

The stability studies using DLS showed that Gal-CLM maintained similar size distribution even after 1000 times dilution (mimicking i.v. injection), whereas two populations were observed for Gal-decorated NCLMs (Gal-NCLM) (Figure 4A). In addition, Gal-NCLM tended to aggregate in the presence of 2 M NaCl, whereas Gal-CLM remained intact (Figure 4B). Both Gal-NCLM and Gal-CLM were shown to be sufficiently stable in the presence of 10% FBS (Figure 4B). Hence, PTX-loaded

interfacially CLMs can be readily prepared with high DLE and superior stability.

In Vitro PTX Release. The in vitro release of PTX from Gal-decorated PTX-loaded CLM (Gal-PTX-CLM) and Gal-decorated PTX-loaded NCLM (Gal-PTX-NCLM) was studied in PB (10 mM, pH 7.4) at 37 °C at micelle concentrations of 0.75 and 0.075 mg/mL, which correspond to ca. 56 and 5.6 μg equiv PTX/mL for Gal-PTX-NCLM and 44 and 4.4 μg equiv PTX/mL for Gal-PTX-CLM, respectively. PTX was reported to have a solubility of ca. 1 μg/mL in PB.[39] To achieve sink conditions, we performed the release studies with 1 mL of PTX-loaded micelles against 25 mL of PB, and at different time intervals, 7 mL of release media was taken and replenished with an equal volume of fresh media. As micelles released PTX slowly, in all cases, PTX concentration in the release media was kept much lower than the maximal solubility of PTX. The results showed that the release of PTX from Gal-PTX-CLM and Gal-PTX-NCLM at 0.75 mg/mL were both slow (ca. 7 and 14% drug released in 94 h, respectively) (Figure 5). Interestingly, at a lower micelle concentration (0.075 mg/mL), the release of PTX from Gal-PTX-CLM remained inhibited, wherein only ca. 25% of drug was released in 94 h (Figure 5), in agreement with their high stability, as previously shown. In contrast, ca. 70% of PTX was released from Gal-PTX-NCLM under otherwise the same conditions. The release studies performed in the presence of 5% FBS showed that serum had practically no influence on release behaviors of Gal-PTX-CLM, whereas slightly faster release of PTX was observed for Gal-PTX-NCLM (Figure 5), further confirming better stability of Gal-PTX-CLM as compared with Gal-PTX-NCLM. Inhibited drug release was also observed for cross-linked PEG-PAC-PCL micelles (without Gal ligands).

It should be noted that loaded drugs would be released instantaneously from the NCL PEG-PCL micelles at a micelle concentration close to or lower than the CMC owing to dissociation of micelles.[31] Here because of limit of detection we were unable to perform the release studies at such low concentration. The current results have, however, indicated that interfacial cross-linking can largely enhance micellar drug stability and may effectively prevent premature drug release following i.v. injection.

Cytotoxicity of Gal-PTX-CLM in HepG2 Cells. The targetability and cytotoxicity of Gal-PTX-CLM were evaluated in hepatocellular carcinoma (HepG2) cells that overexpress asialoglycoprotein receptors. HepG2 cells were treated with PTX-CLM and Gal-PTX-CLM for 24 or 72 h. The dosage was set at 6 μg equiv PTX/mL, similar to our previous report.[35] The cell viability was assessed by MTT assays. The results showed clearly that Gal-decorated PTX-loaded micelles, either cross-linked or non-cross-linked, had much higher cytotoxicity than the corresponding ones without Gal ligands (Figure 6A), supporting the fact that PTX is delivered to HepG2 cells via a receptor-mediated mechanism. For example, cell viabilities of 72 and 48% were observed for HepG2 cells following 24 h of incubation with PTX-CLM and Gal-PTX-CLM, respectively

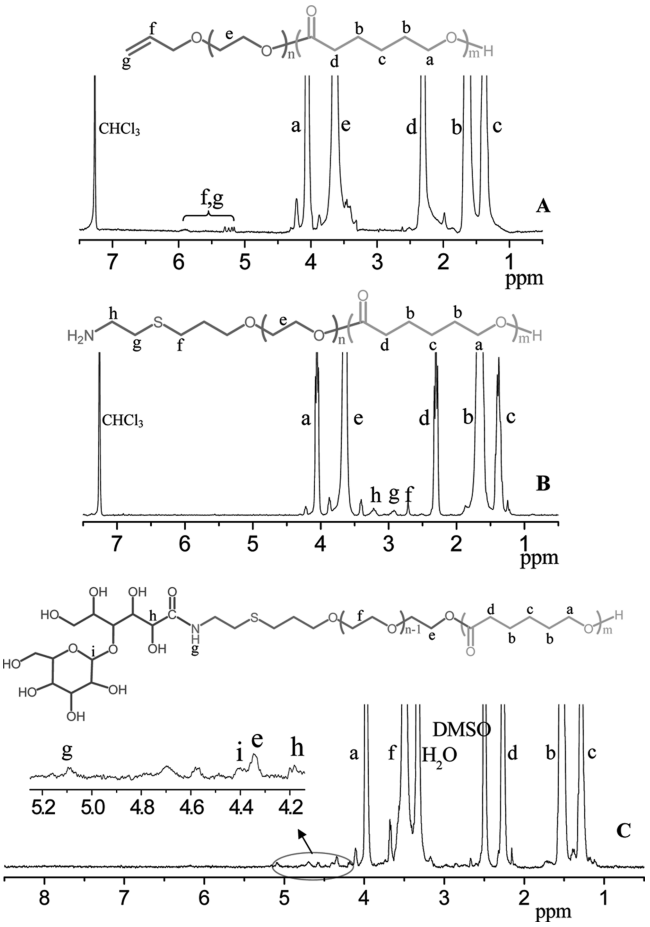

Figure 2. ^{1}H NMR spectra (400 MHz) of allyl-PEG-PCL in $CDCl_3$ (A), NH_2—PEG-PCL in $CDCl_3$ (B), and Gal-PEG-PCL in DMSO-d_6 (C).

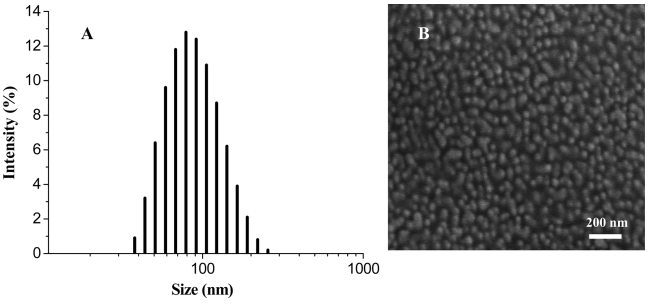

Figure 3. Size distribution of cross-linked micelles containing 20 wt % Gal-PEG-PCL (Gal-CLM) measured by DLS (A) and SEM (B).

Table 2. Average Hydrodynamic Sizes and Zeta Potentials of Non-Crosslinked and Crosslinked Micelles Containing Varying Amounts of Gal-PEG-PCL Copolymer

Gal-PEG-PCL content (wt %)	NCLM			CLM		
	size (nm)	PDI	zeta (mV)	size (nm)	PDI	zeta (mV)
0	87 ± 2.2	0.23	−0.2 ± 0.03	79 ± 0.6	0.12	−2.1 ± 0.02
5	110 ± 1.6	0.22	−1.5 ± 0.02	93 ± 0.3	0.18	−0.9 ± 0.04
10	113 ± 1.8	0.25	0.6 ± 0.04	88 ± 1.0	0.16	−1.6 ± 0.01
15	109 ± 2.5	0.28	0.4 ± 0.03	87 ± 1.1	0.19	−3.1 ± 0.05
20	115 ± 2.8	0.27	1.2 ± 0.01	94 ± 1.7	0.22	−0.9 ± 0.04

Table 3. Characteristics of PTX-Loaded Photo-Cross-Linked Micelles

Gal-PEG-PCL content (wt %)	PTX-NCLM			PTX-CLM			DLC (wt.%)[c]	DLE (%)[c]
	size (nm)[a]	PDI[a]	zeta (mV)[b]	size (nm)[a]	PDI[a]	zeta (mV)[b]		
0	96 ± 1.2	0.11	−0.1 ± 0.01	81 ± 0.5	0.10	−1.5 ± 0.03	7.5	83
5	105 ± 2.0	0.20	0.3 ± 0.04	86 ± 1.6	0.19	−1.4 ± 0.03	7.1	78
10	118 ± 1.6	0.25	0.7 ± 0.02	94 ± 1.4	0.26	−3.5 ± 0.02	6.4	70
15	120 ± 2.8	0.24	0.2 ± 0.03	92 ± 2.0	0.24	−5.3 ± 0.03	6.5	71
20	116 ± 2.4	0.29	1.3 ± 0.02	95 ± 1.3	0.20	−0.8 ± 0.04	5.9	65

[a] Determined by dynamic light scattering (DLS). [b] Determined by zeta potential measurements. [c] Determined by HPLC.

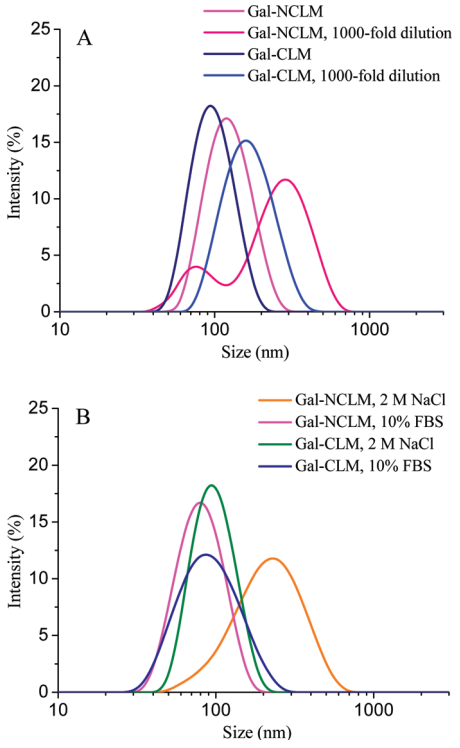

Figure 4. Stability of Gal-CLM and Gal-NCLM against 1000-fold dilution (A) and 2 M NaCl or 10% FBS (B), as measured by DLS at an angle of 173°. The initial micelle concentration was 0.75 mg/mL.

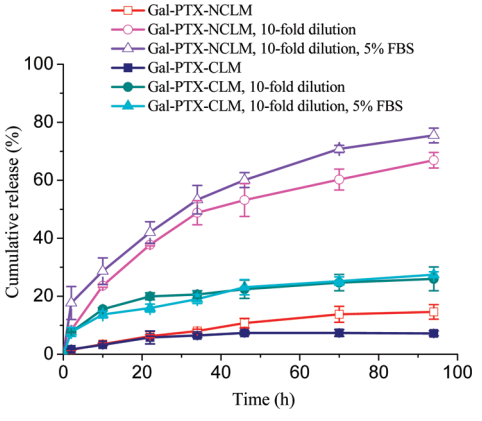

Figure 5. Release of PTX from Gal-PTX-CLM and Gal-PTX-NCLM at pH 7.4 and 37 °C in PB buffer. The initial micelle concentration was 0.75 mg/mL.

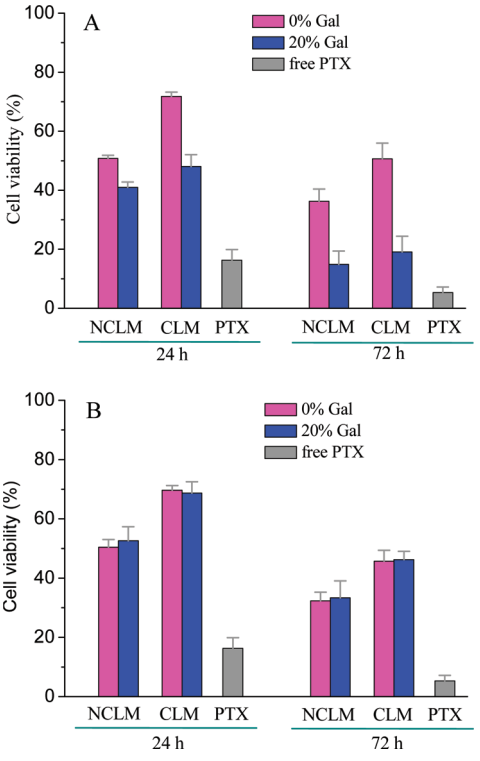

Figure 6. Cytotoxicity of Gal-PTX-CLM, Gal-PTX-NCLM, PTX-CLM, PTX-NLM, and free PTX in HepG2 cells (A) and A549 cells (B). PTX dosage was 6 μg/mL. The cells were incubated with micellar PTX or free PTX for 24 or 72 h. Data are presented as the average ± standard deviation (n = 4).

(Figure 6A). The cell viabilities further decreased with increasing incubation time to 72 h, in which ca. 52 and 18% cells were viable for PTX-CLM and Gal-PTX-CLM, respectively (Figure 6A). The apparent targetability of Gal-decorated micelles could be related to the excellent availability of Gal at the micelle surface to interact with asialoglycoprotein receptors in HepG2 cells because of a longer PEG spacer of Gal-PEG-PCL than that of PEG-PAC-PCL (6.0 versus 5.0 kg/mol). It is noted that Gal-PTX-CLM showed only slightly lower cytotoxicity to HepG2 cells than corresponding Gal-PTX-NCLM (cell viability 18 versus 15% for 72 h incubation). This result is remarkable given the fact that the in vitro drug release from PTX-CLM was significantly inhibited (Figure 5). One possible explanation could be that Gal-decorated micelles are so efficiently taken up by HepG2 cells that a small amount of drug release from micelles is sufficient to induce significant antitumor effect (i.e., drug release is not the deciding step). In general, Gal-decorated

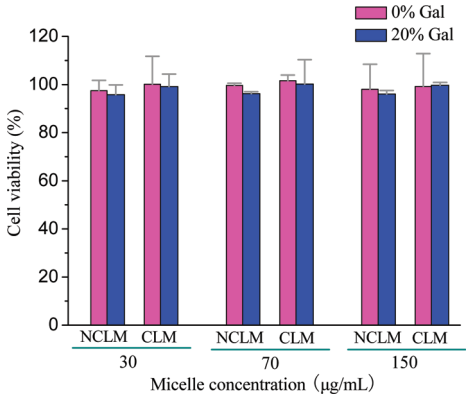

Figure 7. Cytotoxicity of Gal-CLM, Gal-NCLM, and corresponding PEG-PAC-PCL micelles without Gal ligand. HepG2 cells were incubated with micelles for 24 h. Data are presented as the average ± standard deviation (n = 4).

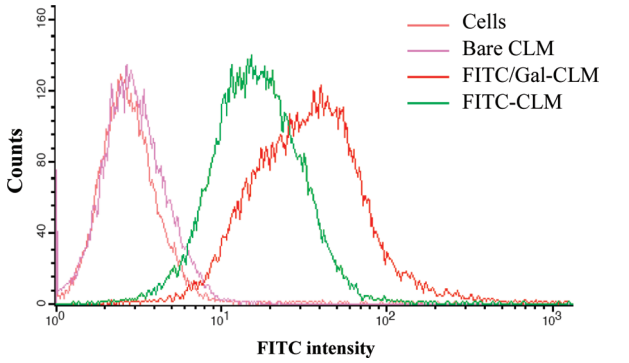

Figure 8. Flow cytometry measurements on cellular internalization of FITC-labeled CLM (FITC-CLM) and FITC-labeled Gal-CLM (FITC/Gal-CLM) into HepG2 cells following 24 h of incubation (micelle concentration 0.2 mg/mL, cell counts 20 000). HepG2 cells and bare micelles (i.e., without FITC label) are used as negative controls.

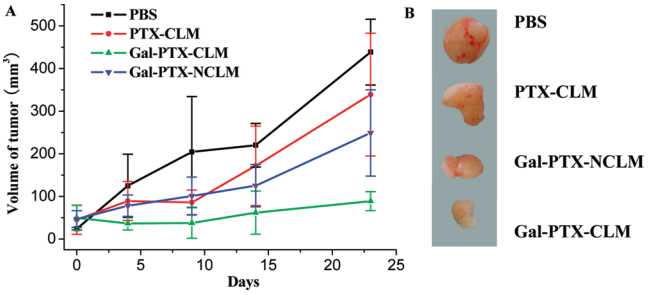

Figure 9. Tumor volume changes of the SMMC-7721 tumor-bearing nude mice after a single i.v. injection of the PTX-loaded micelles via the tail vein on days 0 and 7 (dosage: 3 mg PTX/kg body weight in 0.2 mL PBS) (A) and photographs of tumor blocks of mice sacrificed on day 23 (B).

PTX-loaded micelles, either cross-linked or non-cross-linked, were less cytotoxic than free PTX. It has to be noted, however, that for in vivo applications, it is unlikely that such a high concentration of free PTX or PTX-loaded NCL micelles would be present at the diseased sites for such a long treatment time.

To confirm that Gal-decorated PTX-loaded micelles were taken up by HepG2 cells via a receptor-mediated mechanism, we performed control experiments using A549 cells (without asialoglycoprotein receptors). Notably, the results showed that both Gal-PTX-CLM and Gal-PTX-NCLM had similar cytotoxicity to their counterparts without Gal ligands in A549 cells (Figure 6B). The cell viability of A549 cells was comparable to that observed for HepG2 cells treated with PTX-CLM and PTX-NCLM, whereas it was much higher than that for HepG2 cells treated with Gal-PTX-CLM and Gal-PTX-NCLM under otherwise the same conditions, corroborating active targeting of Gal-PTX-CLM and Gal-PTX-NCLM to HepG2 cells. It should be noted that empty micelles, either with or without Gal ligands, cross-linked or non-cross-linked, were nontoxic to HepG2 cells up to a tested concentration of 150 μg/mL, which is ca. two times that used for the delivery of PTX to HepG2 cells (Figure 7).

The receptor-mediated endocytosis of Gal-CLM into HepG2 cells was further verified by flow cytometry, which has been used for quantitative determination of the cellular uptake of DOX and/or FITC-labeled micelles.[15,40−42] FITC-labeled CL micelles (FITC/Gal-CLM) were obtained by coupling FITC to the surface of the CL micelles consisting of 30 wt % NH_2−PEG-PCL and 20 wt % Gal-PEG-PCL. Interestingly, the results showed that the cellular binding of FITC/Gal-CLM following 24 h incubation was about 3.5-fold higher than that without Gal ligand (Figure 8). This significantly enhanced cellular binding of FITC/Gal-CLM supports that Gal-decorated CL micelles can effectively target to HepG2 cells.

In Vivo Hepatoma-Targeting and Antitumor Efficacy. To evaluate the hepatoma-targeting and antitumor effects of Gal-decorated PTX-loaded CL micelles (Gal-PTX-CLM), we carried out in vivo animal studies using nude mice implanted with SMMC-7721 hepatocytes (human hepatic carcinoma). The liver tumor was shown to be sensitive to PTX therapy.[43] Here three other formulations, that is, PTX-loaded CLMs (PTX-CLM), Gal-decorated PTX-loaded NCLMs (Gal-PTX-NCLM), and PBS were used as controls. The mice were intravenously dosed with 3 mg equiv PTX/kg body weight on days 0 and 7. The dosage was relatively low as compared with most studies (5−50 mg equiv PTX/kg). The progress of tumor volume was monitored over a treatment period of 23 days. Interestingly, the results showed that Gal-PTX-CLM suppressed the tumor growth far more effectively than PTX-CLM and Gal-PTX-NCLM (Figure 9). For example, at day 23, the mice treated with Gal-PTX-CLM had an average tumor volume of ca. 90 mm^3, whereas those treated with PTX-CLM and Gal-PTX-NCLM had much larger tumor volumes of ca. 340 and 250 mm^3, respectively. The mice were sacrificed at day 23, and the tumor blocks were isolated and weighed (Figure 9). The results showed average tumor weights of 0.294, 0.282, 0.216, and 0.091 g for mice treated with PBS, PTX-CLM, Gal-PTX-NCLM, and Gal-PTX-CLM, respectively, further confirming the greatest inhibition of tumor growth by Gal-PTX-CLM. The inferior antitumor efficacy of PTX-CLM was most likely due to their poor cellular uptake by SMMC-7721 cells, signifying the importance of introducing a targeting ligand to micellar drugs. The enhanced antitumor efficacy of Gal-PTX-CLM as compared with Gal-PTX-NCLM highlights the significant role of micelle stabilization.

CONCLUSIONS

We have demonstrated for the first time that galactose-functionalized paclitaxel-loaded interfacially cross-linked biodegradable PEG-PCL block copolymer micelles can effectively

target hepatic tumor cells in vitro as well as hepatoma in vivo, resulting in significantly enhanced antitumor efficacy. The present biodegradable micellar drugs have combined several unique features: (i) they can be readily prepared and cross-linked by UV-irradiation; (ii) they are designed with galactose fully exposing at the surface to accomplish optimal targeting; and (iii) they are highly stable with minimal drug release at low micelle concentrations reflecting the i.v. injection. To the best of our knowledge, this represents the first proof of concept that the in vivo targetability and antitumor efficacy of "traditional" biodegradable micellar drug delivery systems can be markedly enhanced by elegant combination of micelle cross-linking and active targeting. Inspired by the results of this work, we are currently developing different types of tumor-targeting cross-linked biodegradable micellar anticancer drugs. We are convinced that these tumor-targeting robust micelles will have a great potential in targeted cancer chemotherapy.

AUTHOR INFORMATION

Corresponding Author

*Tel/Fax: +86-512-65880098. E-mail: zyzhong@suda.edu.cn.

ACKNOWLEDGMENT

This work is financially supported by research grants from the National Natural Science Foundation of China (NSFC 50703028, 20974073, 50973078, and 20874070), Scientific Research Foundation for Returned Overseas Chinese Scholars (Ministry of Education), a Project Funded by the Priority Academic Program Development of Jiangsu Higher Education Institutions, and the Program of Innovative Research Team of Soochow University.

REFERENCES

(1) Peer, D.; Karp, J. M.; Hong, S.; Farokhzad, O. C.; Margalit, R.; Langer, R. *Nat. Nanotechnol.* **2007**, *2*, 751–760.
(2) Davis, M. E.; Chen, Z.; Shin, D. M. *Nat. Rev. Drug Discovery* **2008**, *7*, 771–782.
(3) van Nostrum, C. F. *Soft Matter* **2011**, *7*, 3246–3259.
(4) Kakizawa, Y.; Kataoka, K. *Adv. Drug Delivery Rev.* **2002**, *54*, 203–222.
(5) Bae, Y.; Kataoka, K. *Adv. Drug Delivery Rev.* **2009**, *61*, 768–784.
(6) Kim, S. C.; Kim, D. W.; Shim, Y. H.; Bang, J. S.; Oh, H. S.; Kim, S. W.; Seo, M. H. *J. Controlled Release* **2001**, *72*, 191–202.
(7) Lee, E. S.; Oh, K. T.; Kim, D.; Youn, Y. S.; Bae, Y. H. *J. Controlled Release* **2007**, *123*, 19–26.
(8) Chen, W.; Meng, F. H.; Li, F.; Ji, S.-J.; Zhong, Z. Y. *Biomacromolecules* **2009**, *10*, 1727–1735.
(9) Sun, H. L.; Guo, B. N.; Cheng, R.; Meng, F. H.; Liu, H. Y.; Zhong, Z. Y. *Biomaterials* **2009**, *30*, 6358–6366.
(10) Matsumura, Y.; Hamaguchi, T.; Ura, T.; Muro, K.; Yamada, Y.; Shimada, Y.; Shirao, K.; Okusaka, T.; Ueno, H.; Ikeda, M.; Watanabe, N. *Br. J. Cancer* **2004**, *91*, 1775–1781.
(11) Kim, T.-Y.; Kim, D.-W.; Chung, J.-Y.; Shin, S. G.; Kim, S.-C.; Heo, D. S.; Kim, N. K.; Bang, Y.-J. *Clin. Cancer Res.* **2004**, *10*, 3708–3716.
(12) Oerlemans, C.; Bult, W.; Bos, M.; Storm, G.; Nijsen, J.; Hennink, W. *Pharm. Res.* **2010**, *27*, 2569–2589.
(13) Tong, R.; Cheng, J. J. *Polym. Rev.* **2007**, *47*, 345–381.
(14) Nasongkla, N.; Shuai, X.; Ai, H.; Weinberg, B. D.; Pink, J.; Boothman, D. A.; Gao, J. M. *Angew. Chem., Int. Ed.* **2004**, *43*, 6323–6327.
(15) Yoo, H. S.; Park, T. G. *J. Controlled Release* **2004**, *96*, 273–283.
(16) Noh, T.; Kook, Y. H.; Park, C.; Youn, H.; Kim, H.; Oh, E. T.; Choi, E. K.; Park, H. J.; Kim, C. *J. Polym. Sci., Polym. Chem.* **2008**, *46*, 7321–7331.
(17) Huang, C. K.; Lo, C. L.; Chen, H. H.; Hsiue, G. H. *Adv. Funct. Mater.* **2007**, *17*, 2291–2297.
(18) Wu, D. Q.; Lu, B.; Chang, C.; Chen, C. S.; Wang, T.; Zhang, Y. Y.; Cheng, S. X.; Jiang, X. J.; Zhang, X. Z.; Zhuo, R. X. *Biomaterials* **2009**, *30*, 1363–1371.
(19) Bae, Y. H.; Yin, H. Q. *J. Controlled Release* **2008**, *131*, 2–4.
(20) Read, E. S.; Armes, S. P. *Chem. Commun.* **2007**, 3021–3035.
(21) O'Reilly, R. K.; Hawker, C. J.; Wooley, K. L. *Chem. Soc. Rev.* **2006**, *35*, 1068–1083.
(22) Rijcken, C. J. F.; Soga, O.; Hennink, W. E.; van Nostrum, C. F. *J. Controlled Release* **2007**, *120*, 131–148.
(23) Huang, H. Y.; Remsen, E. E.; Wooley, K. L. *Chem. Commun.* **1998**, 1415–1416.
(24) Harrisson, S.; Wooley, K. L. *Chem. Commun.* **2005**, 3259–3261.
(25) Cheng, C.; Khoshdel, E.; Wooley, K. L. *Macromolecules* **2007**, *40*, 2289–2292.
(26) Shuai, X. T.; Ai, H.; Nasongkla, N.; Kim, S.; Gao, J. M. *J. Controlled Release* **2004**, *98*, 415–426.
(27) Rijcken, C. J.; Snel, C. J.; Schiffelers, R. M.; van Nostrum, C. F.; Hennink, W. E. *Biomaterials* **2007**, *28*, 5581–5593.
(28) Li, Y.-L.; Zhu, L.; Liu, Z. Z.; Cheng, R.; Meng, F. H.; Cui, J.-H.; Ji, S.-J.; Zhong, Z. Y. *Angew. Chem., Int. Ed.* **2009**, *48*, 9914–9918.
(29) Cheng, C.; Qi, K.; Germack, D. S.; Khoshdel, E.; Wooley, K. L. *Adv. Mater.* **2007**, *19*, 2830–2835.
(30) Talelli, M.; Iman, M.; Varkouhi, A. K.; Rijcken, C. J. F.; Schiffelers, R. M.; Etrych, T.; Ulbrich, K.; van Nostrum, C. F.; Lammers, T.; Storm, G.; Hennink, W. E. *Biomaterials* **2010**, *31*, 7797–7804.
(31) Xu, Y. M.; Meng, F. H.; Cheng, R.; Zhong, Z. Y. *Macromol. Biosci.* **2009**, *9*, 1254–1261.
(32) Xu, H. F.; Meng, F. H.; Zhong, Z. Y. *J. Mater. Chem.* **2009**, *19*, 4183–4190.
(33) Shuai, X.; Merdan, T.; Schaper, A. K.; Xi, F.; Kissel, T. *Bioconjugate Chem.* **2004**, *15*, 441–448.
(34) Talelli, M.; Rijcken, C. J. F.; Oliveira, S.; van der Meel, R.; van Bergen en Henegouwen, P. M. P.; Lammers, T.; van Nostrum, C. F.; Storm, G.; Hennink, W. E. *J. Controlled Release* **2011**, *151*, 183–192.
(35) Xiong, J.; Meng, F.; Wang, C.; Cheng, R.; Liu, Z.; Zhong, Z. *J. Mater. Chem.* **2011**, *21*, 5786–5794.
(36) Chen, W.; Yang, H. C.; Wang, R.; Meng, F. H.; Wei, W. X.; Zhong, Z. Y. *Macromolecules* **2010**, *43*, 201–207.
(37) Bryant, S. J.; Nuttelman, C. R.; Anseth, K. S. *J. Biomater. Sci., Polym. Ed.* **2000**, *11*, 439–457.
(38) Chen, W.; Meng, F. H.; Cheng, R.; Zhong, Z. Y. *J. Controlled Release* **2010**, *142*, 40–46.
(39) Dordunoo, S. K.; Burt, H. M. *Int. J. Pharmaceut.* **1996**, *133*, 191–201.
(40) Upadhyay, K. K.; Bhatt, A. N.; Mishra, A. K.; Dwarakanath, B. S.; Jain, S.; Schatz, C.; Le Meins, J. F.; Farooque, A.; Chandraiah, G.; Jain, A. K.; Misra, A.; Lecommandoux, S. *Biomaterials* **2010**, *31*, 2882–2892.
(41) Zhao, H. Z.; Yue, L.; Yung, L. *Int. J. Pharm.* **2008**, *349*, 256–268.
(42) Xu, P. S.; Van Kirk, E. A.; Zhan, Y. H.; Murdoch, W. J.; Radosz, M.; Shen, Y. Q. *Angew. Chem., Int. Ed.* **2007**, *46*, 4999–5002.
(43) Danhier, F.; Vroman, B.; Lecouturier, N.; Crokart, N.; Pourcelle, V.; Freichels, H.; Jerome, C.; Marchand-Brynaert, J.; Feron, O.; Preat, V. *Biomaterials* **2009**, *140*, 166–173.